Energy 68 (2014) 584–591

Contents lists available at ScienceDirect

Energy

journal homepage: www.elsevier.com/locate/energy

Biodiesel production from soybean and *Jatropha* oils by magnetic $CaFe_2O_4$–$Ca_2Fe_2O_5$-based catalyst

Bao-jin Xue [a,b], Jia Luo [a], Fan Zhang [a,b], Zhen Fang [a,*]

[a] *Chinese Academy of Sciences, Biomass Group, Key Laboratory of Tropical Plant Resource and Sustainable Use, Xishuangbanna Tropical Botanical Garden, 88 Xuefulu, Kunming, Yunnan Province 650223, China*

[b] *University of Chinese Academy of Sciences, 19A Yuquan Road, Beijing 100049, China*

ARTICLE INFO

Article history:
Received 14 October 2013
Received in revised form
17 February 2014
Accepted 20 February 2014
Available online 19 March 2014

Keywords:
Magnetic catalyst
$CaFe_2O_4$
$Ca_2Fe_2O_5$
Biodiesel
Soybean oil
Jatropha oil

ABSTRACT

Heterogeneous $CaFe_2O_4$–$Ca_2Fe_2O_5$-based catalyst with weak magnetism was prepared by co-precipitation and calcination. It was characterized by various techniques including X-ray diffraction, X-ray photoelectron spectroscopy and temperature programmed desorption method. Its active components were identified as mainly Ca–Fe composite oxides such as $CaFe_2O_4$ for transesterification. The magnetism was further strengthened by reducing its component of Fe_2O_3 to Fe_3O_4–Fe under H_2 atmosphere for better magnetic separation. Both catalysts were used for the catalytic transesterification of soybean and *Jatropha* oils to biodiesel. The highest biodiesel yields for soybean oil of 85.4% and 83.5% were obtained over the weak and strong magnetic catalysts, respectively under the optimized conditions (373 K, 30 min, 15/1 methanol/oil molar ratio and 4 wt% catalyst). The catalysts could be recycled three times. Biodiesel production from pretreated *Jatropha* oil was tested with the magnetic $CaFe_2O_4$–$Ca_2Fe_2O_5$–Fe_3O_4–Fe catalyst, and 78.2% biodiesel yield was obtained. The magnetic $CaFe_2O_4$–$Ca_2Fe_2O_5$-based catalyst shows a potential application for the green production of biodiesel.

1. Introduction

Recently, due to the depletion of fossil resources and increased environmental concerns, many studies are seeking for green and renewable fuels to supplement and replace traditional fossil fuels. Biodiesel is considered as one of potential alternative fuels, as it contains less sulfur and it is carbon-neutral, renewable and biodegradable [1–3].

Biodiesel is generally produced by the transesterification of vegetable oils or animal fats with methanol or ethanol in the presence of homogeneous acid and base catalysts such as sulfuric acid and sodium hydroxide [4]. Methanol and ethanol are primarily chosen as alcohol materials, as they are commodity chemicals, with lower price than high-boiling-point alcohols. With methanol and ethanol, the steric hindrance that possibly affects the efficiency of transesterification could be ignored [5]. However, when homogeneous catalysts are used, the issues such as wastewater and emulsification during purification and catalyst separation result in obstacle in operation, reduction in biodiesel yield, and high cost in process [6].

Heterogeneous acid/base catalysts are economic and environmental-friendly because they can be easily recovered and reused [1,7–10]. Especially, some solid magnetic catalysts containing ferrites and Fe/Ni alloys are convenient to be separated from reaction products by a magnet [11–13]. Calcium oxide [6,14,15] or its loading catalysts [16–19] is the most attractive heterogeneous base due to its high catalytic activity and low-cost. But the dissolution/leaching of CaO in methanol or glycerol during the reactions cannot be ignored [11,12]. The amount of soluble substance was reported to be up to 10.5% after the transesterification over CaO in refluxing methanol for 2 h, and most of soluble Ca was determined in the spent glycerin phase [20]. The leaching of CaO results in the loss of catalyst activity, the reduction of catalyst lifetime and additional cost for product purification and catalyst separation. It is expected to be solved by preparing novel Ca–Fe composites such as $CaFe_2O_4$ and $Ca_2Fe_2O_5$ as catalysts. Current method to synthesize $CaFe_2O_4$ and $Ca_2Fe_2O_5$ is mixing CaO or $CaCO_3$ with Fe_2O_3 powders in certain proportions and calcinating at 1273 K for 3–24 h [21,22]. The prepared catalysts exhibited high activity and structural stability in the selective oxidation of styrene [23] and combustion of propylene [22]. $Ca_2Fe_2O_5$ prepared by the calcination of Fe_2O_3/$CaCO_3$ mixture at 1323 K showed high activity for the transesterification of rapeseed oil to biodiesel, but it was easy to be deactivated [24].

---

[*] Corresponding author. Tel.: +86 871 65137468; fax: +86 871 65160916.
E-mail addresses: zhenfang@xtbg.ac.cn, zhen.fang@mail.mcgill.ca (Z. Fang).
URL: http://brg.groups.xtbg.ac.cn/

http://dx.doi.org/10.1016/j.energy.2014.02.082
0360-5442/© 2014 Elsevier Ltd. All rights reserved.

In this work, magnetic $CaFe_2O_4$–$Ca_2Fe_2O_5$-based catalyst was synthetized by co-precipitation, calcination and reduction, and used in the transesterification of soybean and *Jatropha* oils to biodiesel in the presence of methanol. The active components of these heterogeneous catalysts were identified as calcium ferrites, namely $CaFe_2O_4$ and $Ca_2Fe_2O_5$. Various technologies were used to characterize these catalysts, and clarify their activities. The catalyst is expected to be more thermal stable than single CaO catalyst, and could be magnetically recovered from the reaction products for the next catalytic run.

2. Experimental

2.1. Materials

Reagents $Ca(NO_3)_2\cdot 4H_2O$, $Fe(NO_3)_3\cdot 9H_2O$, urea, KOH and dehydrated methanol were purchased from Xilong Chemical Factory Co., Ltd., Guangzhou, Guangdong. $Ca(NO_3)_2\cdot 4H_2O$, $Fe(NO_3)_3\cdot 9H_2O$, urea and dehydrated methanol were of analytical grade (purity $\geq$ 98.5–99.5%), while the purity of KOH was 85%. Standard HAME (heptadecanoic acid methyl ester) and methyl esters (of palmitate, linolenate, stearate, oleate, linoleate and linolenate) were purchased from Sigma (Shanghai), with purity $\geq$99%. Soybean oil (acid value of 0.7) was bought from a local supermarket. *Jatropha Curcas L.* oil (acid value of 12.8) was obtained from Xishuangbanna Tropical Botanical Garden, Yunnan.

2.2. Preparation and characterization of catalysts

Aqueous solution (300 mL) of 0.l M $Ca(NO_3)_2$ and 0.1 M $Fe(NO_3)_3$ was prepared in a three-neck flask. Solid urea (1.5 M) was added into the flask. The flask was then submerged in an oil bath at 408 K with mechanical stirring at 200 rpm for 12 h, and subsequently settled at 368 K for 12 h. The formed precipitates together with their mother liquor were transferred to a 1000-mL conical beaker, and washed thoroughly (6–8 times) with deionized water. The solid product was filtered, dried at 353 K for 48 h in a vacuum drier, and ground to powders in a mortar. The powders were calcined at 1073 K for 5 h in a muffle furnace, and $CaFe_2O_4$–$Ca_2Fe_2O_5$–Fe_2O_3 catalyst was obtained. Then the catalyst was used to catalyze transesterification of soybean oil for the production of biodiesel. After reaction, the catalyst was separated by centrifugation, washed with methanol, activated (calcined) at 1073 K for 3 h and recycled as catalyst for transesterification. The $CaFe_2O_4$–$Ca_2Fe_2O_5$–Fe_2O_3 catalyst was also reduced to $CaFe_2O_4$–$Ca_2Fe_2O_5$–Fe_3O_4–Fe catalyst at 773 K under H_2 atmosphere to further improve its magnetism for magnetic separation from biodiesel products.

The structure, morphology and specific surface area of synthesized samples were characterized by X-ray diffraction (XRD, Rigaku TTR3, Tokyo) with a Cu Kα radiation (40 kV and 200 mA), scanning electron microscopy (SEM, Quanta 200, Hillsboro, OR), and Brunauer–Emmett–Teller method (BET, Tristar II 3020, Micromeritics Instruments, Atlanta, GA) with N_2 adsorption, respectively. Surface and bulk elemental compositions of catalysts were determined by X-ray photoelectron spectroscopy (XPS, XSAM800, Kratos Analytical, Inc., NY), energy-dispersive X-ray spectrometry (EDX, Quanta 200, Hillsboro, OR) and inductively coupled plasma-atomic emission spectrometry (ICP-AES, iCAP6300, Thermo Fisher Scientific, Waltham, MA). The magnetic properties were measured at room temperature by vibrating swatch gaussmeter (VSM, HH-15, Nanjing Nanda Instrument Plant, Jiangsu). Surface acidity and basicity were measured by TPD (temperature programmed desorption) using a ChemBET Pulsar TPR/TPD (Quanta, Hillsboro, OR). In TPD analysis, 0.1 g sample was exposed to a He-stream at 423 K for 0.5 h. Then it was flushed with pure CO_2 (or NH_3) gas (50 mL/min) at 373 K for 1 h. After that, the sample was cooled to room temperature, and subsequently desorbed by heating to 1173 K at a heating rate of 10 K/min in a He-stream (50 mL/min).

2.3. Transesterification reaction

Catalytic transesterification of soybean and *Jatropha* oils with dehydrated methanol was conducted in a 300-mL high-pressure autoclave (FCFD05-30, Yantai Jianbang Chemical Mechanical Co. Ltd., Shandong) under N_2 atmosphere. Crude oil (30 g), dehydrated methanol (methanol/oil molar ratio of 12/1–16/1) and $CaFe_2O_4$–$Ca_2Fe_2O_5$–Fe_2O_3 catalyst (3–7 wt%) were loaded in the autoclave. The autoclave was pressurized with N_2 to 1 MPa to avoid methanol evaporation to the dead volume. It was heated slowly to 333–393 K within 30–50 min. Transesterification was carried out at 333–393 K for 5–60 min with stirring at 200 rpm. The actual pressure in the reactor was 1.4–3.0 MPa during the reaction, which was greater than the saturated vapor pressure of methanol at the corresponding temperatures. After reaction, product mixture was transferred to polypropylene tubes and centrifuged at 15,000 rpm for 10 min (3–30 K, Sigma Zentrifugen GmbH, Osterode am Harz, Germany). Three layers, the upper (biodiesel), middle (glycerol and methanol) and bottom (catalyst) layers were formed and separated. The separated catalyst was washed with methanol, calcined at 1073 K for 3 h and recycled as catalyst for the next reaction. Unlike $CaFe_2O_4$–$Ca_2Fe_2O_5$–Fe_2O_3 catalyst, magnetic $CaFe_2O_4$–$Ca_2Fe_2O_5$–Fe_3O_4–Fe catalyst was easily separated by a strong NdFeB magnet after reaction. It was then washed with methanol and dried at 353 K in a vacuum drier for recycles.

Biodiesel was analyzed by gas chromatography (GC; GC-2014, Shimadzu, Japan) with capillary column of Rtx-wax (30 m × ø0.25 mm × 0.25 μm). The column temperature was 493 K, injector temperature was 533 K and detector temperature was 553 K. Carrier gas was helium with flow rate of 0.8 mL/min. The split ratio was 20/1. Biodiesel yield was determined with external standard method.

Two soybean and *Jatropha* biodiesel samples produced with 1 wt% KOH were calibrated and used as external calibrants. First, they were calibrated by HAME using the following equation [25]:

$$Y(\%) = \frac{A_K \times m_I}{A_I \times m_K} \times 100\% \tag{1}$$

where $Y(\%)$ was the biodiesel yield in calibrants; A_K and A_I were GC peak areas of calibrants and HAME, respectively; m_I and m_K were masses of HAME and calibrants, respectively.

Second, relative response factors (the ratio coefficients of GC peak area/sample mass) of six standard methyl esters [oleate (C18: 1), linoleate (C18: 2), palmitate (C16: 0), tearate (C18: 0), linolenate (C16: 1) and linolenate (C18: 3)] to that of HAME (C17: 0) were separately calibrated in GC analysis (Table S1). The biodiesel yield (Y%) was further calibrated using the six coefficients for each peak, 81.5% for soybean and 85.8% for *Jatropha* biodiesel calibrants were obtained, respectively.

Third, the biodiesel yield produced with solid catalysts was calibrated by the calibrants and calculated using the following equation:

$$\text{Biodiesel yield (wt\%)} = \frac{\mathrm{Y}(\%) \times m'_K \times A_E}{m_E \times A'_K} \times 100\% \tag{2}$$

In equation (2), $A'_K$and A_E were peak areas of biodiesel produced by 1% KOH (calibrant) and solid catalysts; m'_K and m_E were masses of biodiesel produced by 1% KOH (calibrant) and solid catalysts, respectively.

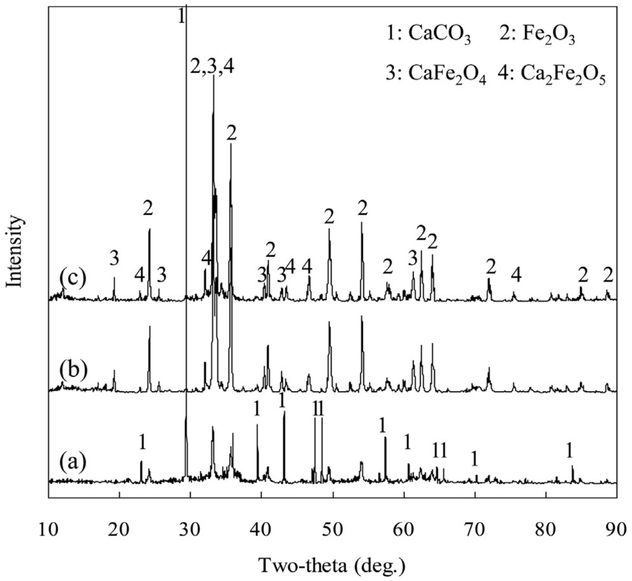

Fig. 1. XRD patterns of $CaFe_2O_4$–$Ca_2Fe_2O_5$–Fe_2O_3 catalyst. (a) un-calcined sample, (b) fresh catalyst, and (c) catalyst after 5 cycles.

3. Results and discussion

3.1. Characterization of $CaFe_2O_4$–$Ca_2Fe_2O_5$–Fe_2O_3 catalyst

3.1.1. XRD And ICP-AES

The crystalline phases of metal oxides in catalyst were determined by XRD (Fig. 1) and compared with the cards from Joint Committee on Powder Diffraction Standards (JCPDS). Un-calcined sample was mainly composed of $CaCO_3$ and Fe_2O_3 (Fig. 1a), and was transformed to a mixture of crystalline $CaFe_2O_4$, $Ca_2Fe_2O_5$ and Fe_2O_3 ($CaFe_2O_4$–$Ca_2Fe_2O_5$–Fe_2O_3) after calcination at 1073 K for 5 h (Fig. 1b). The conversion equations in calcination were described as follows:

$$CaCO_3 \rightarrow CaO + CO_2 \tag{3}$$

$$CaO + Fe_2O_3 \rightarrow CaFe_2O_4 \tag{4}$$

$$2CaO + Fe_2O_3 \rightarrow Ca_2Fe_2O_5 \tag{5}$$

The Ca/Fe molar ratio of bulk catalyst was determined by dissolving it (95.1 mg) in nitrohydrochloric acid (33.3 mL HNO_3–HCl mixture, volume ratio of 1:3) and analyzed by ICP-AES. Result showed that the Ca/Fe molar ratio of calcined catalyst was 0.48, smaller than the stoichiometric ratio of 1.0 in the precursor solution because part of Ca was washed out before calcination.

It was speculated that Fe_2O_3, CaO, and Ca–Fe composite oxides might contribute to the transesterification activity of the solid catalyst. However, un-calcined sample and pure Fe_2O_3 were tested with little biodiesel production. Although CaO might be the high active composition for the transesterification reaction, the concentration of CaO in the solid catalyst was low. No crystal peak of CaO appeared in the XRD pattern for calcined catalyst (Fig. 1b). On the other hand, considering the water-soluble specialty of CaO in water, we washed the calcined catalyst (53.5 mg) with 100 mL water, while the contents of Ca and Fe in the washing water were determined by ICP as only 4.1 wt% and <0.6 wt% of the catalyst weight, respectively. This demonstrated that the active components of the prepared catalyst should be $CaFe_2O_4$ and $Ca_2Fe_2O_5$. The crystalline structure of $CaFe_2O_4$ and $Ca_2Fe_2O_5$ was rather stable after five catalytic cycles (Fig. 1c).

3.1.2. XPS, SEM and EDX

XPS results (Table 1) show that the surface Ca/Fe molar ratio of $CaFe_2O_4$–$Ca_2Fe_2O_5$–Fe_2O_3 catalyst was 0.39, which was lower than that in bulk phase (0.48) by ICP. This demonstrates that more Fe element was concentrated at the surface of solid catalyst. As the Ca/Fe ratio of $CaFe_2O_4$ and $Ca_2Fe_2O_5$ and Fe_2O_3 were 0.5, 1.0 and 0, respectively, the surface composition of the prepared catalyst might be mainly the mixture of $CaFe_2O_4$ and Fe_2O_3

SEM results confirm the analysis with XPS methodology. Clusters of rough particles in un-calcined sample with the particle size of about 20–100 nm (Fig. 2a) were transformed to two types of particles with different morphologies in Fig. 2b (particle A: 200 nm; particle B: 1–2 μm) after calcination. The morphology of catalyst slightly changed after 5 cycles (Fig. 2c). EDX spectrum shows that particle A had Ca/Fe/O molar ratio of 0.10/0.92/1.90, indicating that it was mainly composed of Fe_2O_3 with fewer $CaFe_2O_4$ or $Ca_2Fe_2O_5$. Particle B had Ca/Fe/O molar ratio of 1.00/2.17/5.85, which indicated that it was mainly composed of $CaFe_2O_4$ with fewer Fe_2O_3

3.1.3. BET

The BET specific surface area of un-calcined samples was 95.7 m^2/g, but decreased significantly to 7.8 m^2/g after calcination. The sharp decline was due to the formation of new crystalline phases (mainly $CaFe_2O_4$ and $Ca_2Fe_2O_5$, Fig. 1) and the growth of particle size (Fig. 2b). The surface area was slightly decreased to 5.7 m^2/g after 5 cycles of transesterification reaction.

3.1.4. TPD

The TPD profiles of fresh catalyst (Fig. S1) had two major peaks at 670–800 K and 900–1000 K for CO_2 desorption, with base amounts of 0.026 and 0.01 mmol/g, respectively. These two peaks could be classified both as strong basic sites. The base amount over the weaker basic site (TPD peak of 670–800 K) decreased by 38.5% after 5 cycles, while the base amount over the other basic site kept constant. Similarly, in NH_3-TPD profiles, two acidic sites were

Table 1
Surface Ca/Fe molar ratio of catalysts by XPS analysis.

Catalyst types	Element	Area (cps)	Sensitivity factor	Content (at%)	Molar ratio of Ca/Fe
$CaFe_2O_4$–$Ca_2Fe_2O_5$–Fe_2O_3 catalyst	Ca	1279.5	1.58	9.47	0.39
	Fe	4176.2	2	24.42	
	O	3730.2	0.66	66.11	
$CaFe_2O_4$–$Ca_2Fe_2O_5$–Fe_3O_4–Fe catalyst	Ca	925.3	1.58	9.14	0.35
	Fe	3363.8	2	26.24	
	O	2733.1	0.66	64.62	
Reused $CaFe_2O_4$–$Ca_2Fe_2O_5$–Fe_3O_4–Fe catalysts	Ca	584.9	1.58	6.28	0.27
	Fe	2708.7	2	22.96	
	O	2754.8	0.66	70.76	

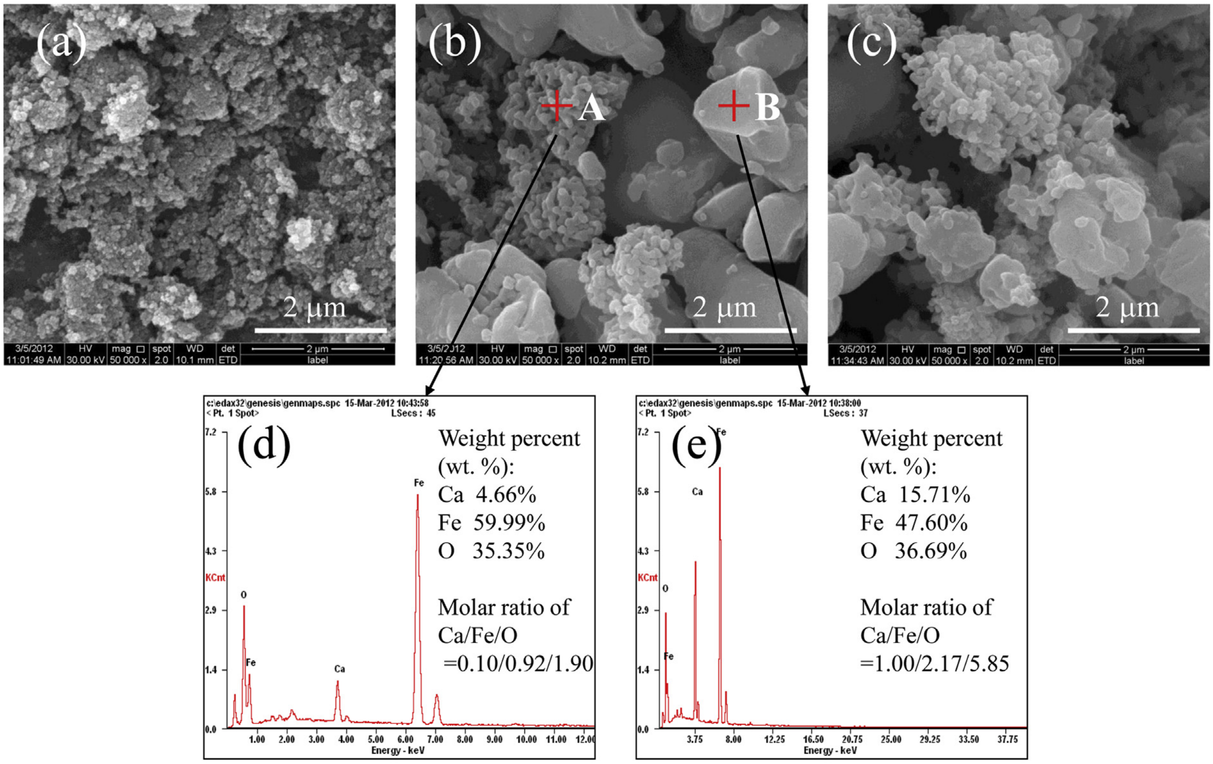

Fig. 2. SEM images and EDX spectra of $CaFe_2O_4$–$Ca_2Fe_2O_5$–Fe_2O_3 catalyst. (a) SEM, un-calcined catalyst, (b) SEM, calcined catalyst, (c) SEM, catalyst after 5 cycles, (d) EDX, particle A in Fig. 2b, and (e) EDX, particle B in Fig. 2b.

detected over the fresh catalyst with the TPD peaks at 670–800 K and 900–1000 K. The acid amounts of these two acidic sites were 0.064 and 0.024 mmol/g, respectively. The acid amount over the acidic site with TPD peak of 670–800 K decreased from 0.064 to 0.034 mmol/g after 5 cycles, while the acid amount over the other strong acidic site kept constant.

3.1.5. VSM

The coercivity (Hc) and specific saturation magnetization (Ms) values of $CaFe_2O_4$–$Ca_2Fe_2O_5$–Fe_2O_3 catalyst (Fig. S2) were 31.44 kA m^{-1} and 0.217 Am^2 kg^{-1} for the fresh catalyst, and 23.66 kA m^{-1} and 0.973 Am^2 kg^{-1} after the fifth catalytic cycle, respectively. After 5 cycles, the magnetism of catalyst increased due to the reduction of Fe_2O_3 to Fe_3O_4 (or Fe) by glycerol residue remained on catalyst during its re-activation (re-calcination) for the next reaction.

3.2. Effects of transesterification process variables

Variables of reaction temperature (333–393 K), reaction time (5–60 min), methanol/oil molar ratio (12/1–16/1) and catalyst amount (3–7 wt% of oil) were studied for the transesterification of soybean oil to biodiesel by single factor test. Results are given in Fig. 3.

3.2.1. Temperature

The influence of reaction temperature was studied at given conditions. Referred to previous works, methanol/oil molar ratio of 15/1 [12,17,26], catalyst of 4 wt% [13,15] and reaction time of 60 min [25,27] were used and fixed in the experiments. At low temperatures ($\leq$343 K), no biodiesel was produced. At high temperature of 393 K, biodiesel yield reached 81.8% in just 5 min. So, temperature in the range of 353–393 K with 10 K interval was used to study its effect on biodiesel yield. In Fig. 3a, the yield was sharply improved from 10.1% to the maximum value of 85.4% as temperature increased from 353 to 373 K, and gradually decreased to 80.0% at 393 K. High temperature improved the catalytic activity of solid catalyst, and therefore benefited higher biodiesel yield. But liquid methanol vaporized into gas phase at much higher temperature, and resulted in poor contact of liquid methanol with soybean oil [15]. Therefore, in this work, the best temperature was 373 K.

3.2.2. Time

Under the given conditions (373 K, methanol/oil molar ratio of 15/1, 4 wt% catalyst), biodiesel yield was almost unchanged (85.1–85.8%) when reaction time decreased from 60 to 40 min. So, reaction time ranged from 10 to 50 min with 10 min interval was used to optimize biodiesel yield. In Fig. 3b, biodiesel yield increased from 22.8% at 10 min to 85.4% at 30 min. As reaction time increased further from 30 to 50 min, biodiesel yield was almost unchanged because reactions had reached the equilibrium [13,15]. Hence, the best reaction time was selected as 30 min.

The effect of temperature and time on biodiesel yield was combined and studied. The effect of reaction temperature (353–393 K, interval 10 K) was studied again at the fixed time of 30 min, not 60 min, while other conditions kept the same (methanol/oil molar ratio of 15/1 and 4 wt% catalyst). The best reaction temperature was again as 373 K, with the highest biodiesel yield of 85.4%.

3.2.3. Methanol/oil molar ratio

Effects of methanol/oil molar ratio from 12/1 to 16/1 on biodiesel yield were studied at 373 K for 30 min with 4 wt% catalyst. Higher methanol/oil molar ratio is required due to the vaporization of methanol at high temperature [13,15]. In Fig. 3c, biodiesel yield increased from 72.7% to 85.4% as methanol/oil molar ratio rose from

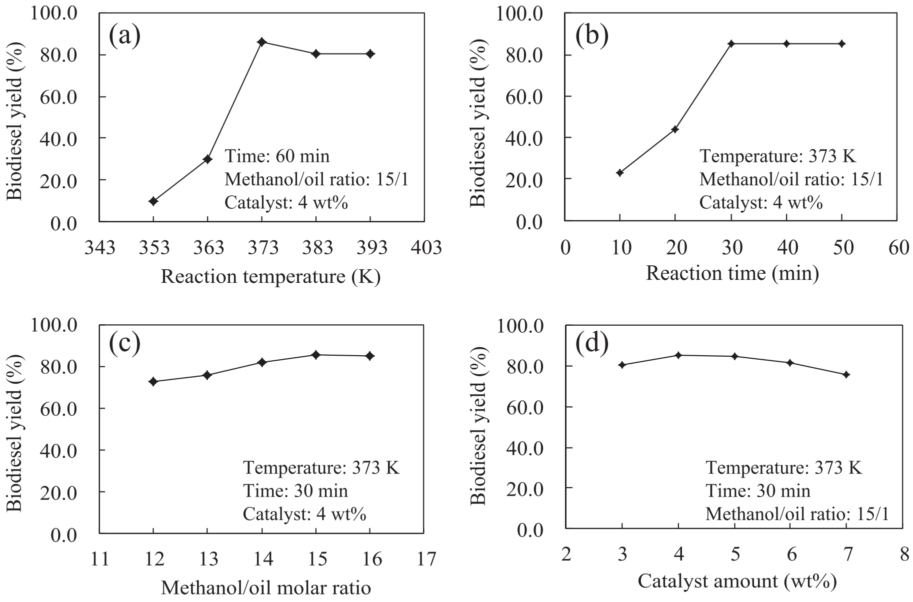

Fig. 3. Effects of variables on biodiesel yields from soybean oil over $CaFe_2O_4$–$Ca_2Fe_2O_5$–Fe_2O_3 catalyst: (a) reaction temperature, (b) reaction time, (c) methanol/oil molar ratio, and (d) catalyst amount.

12/1 to 15/1. Biodiesel yield changed little with the molar ratio rose of 15/1 and 16/1. So, the best methanol/oil molar ratio was 15/1.

3.2.4. *Catalyst amount*

The amount of solid catalyst had also remarkable influence on the improvement of biodiesel yields. For example, the tested amount of CaO catalyst should be higher than 4 wt% to reach a considerable biodiesel yield of >70% from soybean oil [15]. For CaO/α-Fe catalyst, the tested catalyst amount was 4–6 wt%, and the best biodiesel yield occurred at catalyst amount of 6 wt% [13]. Therefore, referred to these published literature, the influence of catalyst amount in the range of 3–7 wt% of soybean oil was studied in this work for biodiesel production at 373 K for 30 min, with methanol/oil molar ratio of 15/1. In Fig. 3d, biodiesel yield increased from 80.4% to 85.4% as catalyst amount rose from 3 to 4 wt%. However, as catalyst increased further from 4 to 7 wt%, biodiesel yield dropped from 85.4% to 75.6%, which was possibly due to the difficult mixing of liquid reactants with high concentration of solid catalyst [15]. Furthermore, an excessive amount of catalyst would lead to the saponification of biodiesel. So the catalyst amount was selected as 4 wt%.

In conclusion, the best conditions to transesterify soybean oil to biodiesel with $CaFe_2O_4$–$Ca_2Fe_2O_5$–Fe_2O_3 catalyst were reaction temperature of 373 K, reaction time of 30 min, methanol/oil molar ratio of 15/1 and catalyst of 4 wt%. Under these conditions, 85.4% biodiesel yield was obtained.

3.3. *Recycle of $CaFe_2O_4$–$Ca_2Fe_2O_5$–Fe_2O_3*

The stability and reusability of catalyst are the most important features for practical applications. The $CaFe_2O_4$–$Ca_2Fe_2O_5$–Fe_2O_3 catalyst was cycled 5 times to test its stability under the best reaction conditions: 373 K, 30 min, methanol/oil molar ratio of 15/1 and catalyst of 4 wt%. Biodiesel yield decreased slightly from 85.4% to 78.6% at the third cycle. At the fourth and fifth cycles, biodiesel yield decreased rapidly to 63.9% and 47.4%, respectively (Fig. 4). Deactivation of the catalyst was caused by three possible reasons: (1) Catalyst active sites were leached because the amounts of strong bases and acids decreased by 38.5% and 46.9% after 5 cycles, respectively (Section 3.1.4); (2) Catalyst aggregated after cycles (Fig. 2b *vs.* 2c); and (3) Char and products deposited on the catalyst. Similar deactivation of solid catalysts was also reported in the catalytic transesterification of pretreated *Jatropha* oil over Mg–Al metal oxides in our previous work, which showed remarkable adsorption of glycerol on catalyst surface and partly leaching of active components into the solution [28].

3.4. *Characterization and reaction with $CaFe_2O_4$–$Ca_2Fe_2O_5$–Fe_3O_4–Fe*

3.4.1. *Strengthening magnetism*

According to Fig. 5 and VSM measurement (Fig. S2), the magnetism of $CaFe_2O_4$–$Ca_2Fe_2O_5$–Fe_2O_3 catalyst was too weak to be separated by a normal magnet. Therefore, nonmagnetic Fe_2O_3 contained in the catalyst was reduced to magnetic Fe_3O_4 or Fe to strengthen the magnetism. Generally, Fe_2O_3 is reduced by hydrogen to Fe_3O_4 at 563–583 K, and part of Fe_3O_4 is further converted to Fe at ≥578 K [29]. Higher temperatures were reported to reduce Fe_2O_3 to Fe_3O_4 by H_2 at 713–763 K, and to Fe at ≥843 K

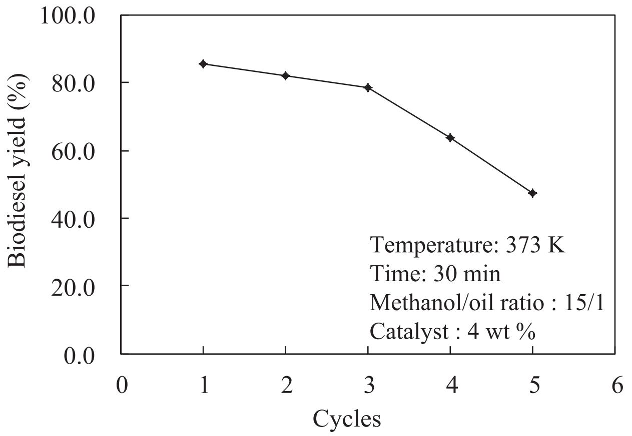

Fig. 4. Biodiesel yield *vs.* catalyst cycles for soybean oil over $CaFe_2O_4$–$Ca_2Fe_2O_5$–Fe_2O_3 catalyst.

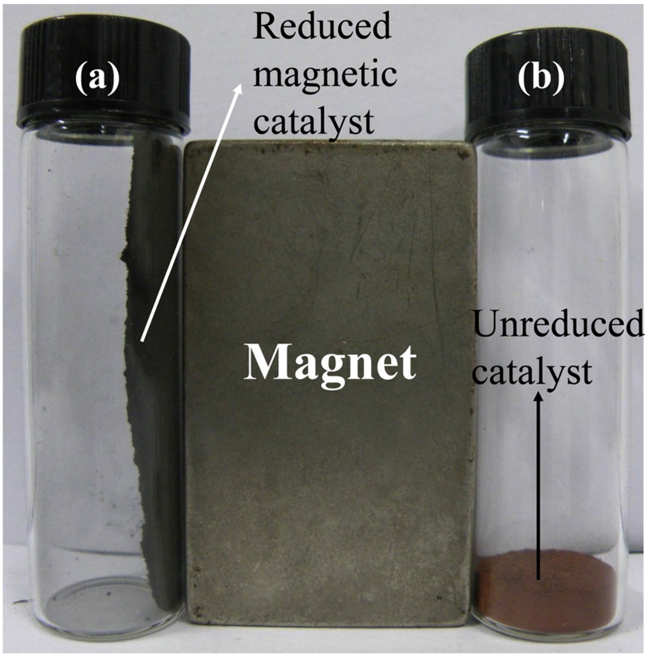

Fig. 5. Images of catalysts with a magnet. (a) $CaFe_2O_4$–$Ca_2Fe_2O_5$–Fe–Fe_3O_4, reduced by 25 vol. % H_2 at 773 K for 180 min; (b) fresh $CaFe_2O_4$–$Ca_2Fe_2O_5$–Fe_2O_3.

[30]. The reduction of catalyst is determined by temperature, gas velocity, catalyst morphology and reduction time. The conversions of Fe_2O_3 to Fe_3O_4 and Fe are summarized as [29,30]

$$3Fe_2O_3 + H_2 \rightarrow 2Fe_3O_4 + H_2O\uparrow \tag{6}$$

$$Fe_3O_4 + 4H_2 \rightarrow 3Fe + 4H_2O\uparrow \tag{7}$$

$$3CaFe_2O_4 + H_2 \rightarrow 2Fe_3O_4 + 3CaO + H_2O\uparrow \tag{8}$$

$$3Ca_2Fe_2O_5 + H_2 \rightarrow 2Fe_3O_4 + 6CaO + H_2O\uparrow \tag{9}$$

In this work, 573 K and 773 K were selected to reduce $CaFe_2O_4$–$Ca_2Fe_2O_5$–Fe_2O_3 catalyst by H_2. The reduction procedure was as follows: $CaFe_2O_4$–$Ca_2Fe_2O_5$–Fe_2O_3 catalyst (2 g) was put in a sealed tubular furnace with pure N_2 flowing (150 mL/min) for 30 min, then N_2 was replaced by H_2 stream (25 vol%, 200 mL/min). The sample was heated to 573 K (or 773 K) in 120 min and kept at 573 K (or 773 K) for 180 min. After cooling, reduced catalyst was obtained. It presented weak magnetism if reduced at low temperature of 573 K. High temperature 773 K was used, reduced catalyst was easily attracted by a magnet with its color changed from brown-red to black (in web version) (Fig. 5).

3.4.2. Characterization of $CaFe_2O_4$–$Ca_2Fe_2O_5$–Fe_3O_4–Fe catalyst

XRD spectrum (Fig. 6a) shows that the reduced catalyst was mainly composed of $CaFe_2O_4$, $Ca_2Fe_2O_5$, Fe and Fe_3O_4. After 3-h reduction course and three catalytic runs, the crystalline structure of active components $CaFe_2O_4$ and $Ca_2Fe_2O_5$ was still stable, and was not reduced (Fig. 6). The reductive Fe and Fe_3O_4 mainly came from Fe_2O_3, not $CaFe_2O_4$ nor $Ca_2Fe_2O_5$

The surface elemental compositions of fresh and reused $CaFe_2O_4$–$Ca_2Fe_2O_5$–Fe_3O_4–Fe catalyst were determined by XPS. The surface Ca/Fe molar ratio of catalyst after reduction was decreased from 0.39 to 0.35 (Table 1). However, the main chemical compositions over the catalyst surface were still $CaFe_2O_4$ and iron oxides, and the active component was still $CaFe_2O_4$

The valence distributions of element Fe were changed after the reduction of $CaFe_2O_4$–$Ca_2Fe_2O_5$–Fe_2O_3 catalyst. The XPS spectra of Fe were deconvolved into five peaks by XPSPEAK95 software (Version 3.1, freeware by Raymund W.M. Kwok, The Chinese University of Hong Kong), which were positioned at binding energy of 723.1–723.4, 716.4–716.9, 710.3–710.5, 709.3–709.5 and 707.0 eV, and were attributed to 2p 1/2, satellite peak of 2p 2/3, 2p 2/3 of Fe^{3+}, 2p 2/3 of Fe^{2+} and 2p 2/3 of Fe^0, respectively (Fig. S3) [31–33]. The 2p 2/3 peak of Fe in the $CaFe_2O_4$–$Ca_2Fe_2O_5$–Fe_2O_3 catalyst was positioned at binding energy of 710.3 eV, which implied that the Fe contained in the catalyst was mainly trivalent Fe^{3+}. After the reduction to $CaFe_2O_4$–$Ca_2Fe_2O_5$–Fe_3O_4–Fe catalyst, the 2p 2/3 peak of Fe in the catalyst shifted to lower binding energy of 709.3 and 707.0 eV, which demonstrated that the Fe_2O_3 was converted to Fe_3O_4 and Fe in the reduced catalyst.

Solid catalyst possibly produced some CaO during the reduction of catalyst (section 3.4.1, equations (8) and (9)). However, experiments demonstrated that less CaO was produced during this course. The water-soluble Ca content in the reduced catalyst (analyzed by ICP) was only 4.6 wt%, which was a little higher than that of unreduced catalyst (4.1 wt%).

3.4.3. Transesterification of soybean oil over $CaFe_2O_4$–$Ca_2Fe_2O_5$–Fe_3O_4–Fe

The transesterification of soybean oil over magnetic $CaFe_2O_4$–$Ca_2Fe_2O_5$–Fe_3O_4–Fe catalyst was tested by an orthogonal design. A $L_9(3^4)$ orthogonal table was designed for optimization (Table 2). The four factors were reaction temperature (A: 353, 373, 393 K), reaction time (B: 20, 30, 40 min), methanol to oil molar ratio (C: 13/1, 15/1, 17/1) and catalyst (D: 2, 4, 6 wt%). The impact of these four factors on biodiesel yield followed the order of $A >> B > C \approx D$, and the optimal level combination through the mathematical processing of Table 2 was $A_2B_2C_2D_2$. The optimal conditions for transesterification of soybean oil over $CaFe_2O_4$–$Ca_2Fe_2O_5$–Fe_3O_4–Fe catalyst were 373 K, 30 min, methanol to oil molar ratio of 15/1 and catalyst of 4 wt%, which was consistent with the single factor test results over $CaFe_2O_4$–$Ca_2Fe_2O_5$–Fe_2O_3 catalyst. But, the optimal conditions did not appear in Table 2, as the orthogonal optimization is a

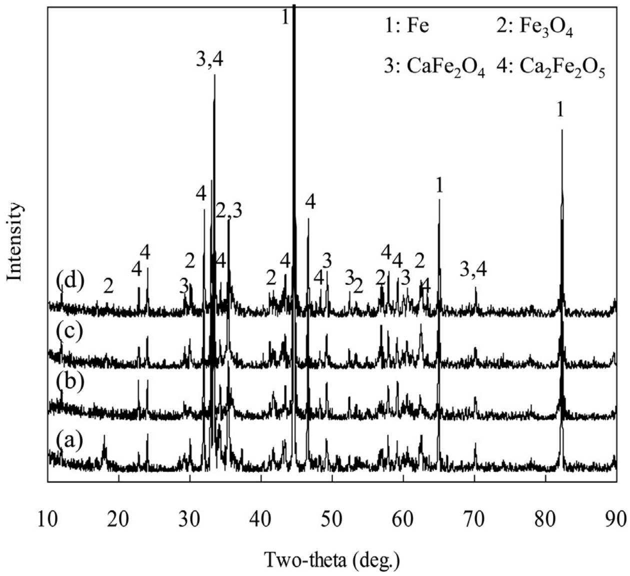

Fig. 6. XRD patterns of magnetic $CaFe_2O_4$–$Ca_2Fe_2O_5$–Fe_3O_4–Fe catalyst: (a) fresh, (b) after 1st cycle, (c) after 2nd cycle, (d) after 3rd cycle.

Table 2
Intuitive analysis of transesterification of soybean oil with magnetic $CaFe_2O_4$–$Ca_2Fe_2O_5$–Fe_3O_4–Fe catalyst.

Test#	A reaction temperature (K)	B reactiontime (min)	C Methanol to oil molar ratio (mol/mol)	D Catalyst amount (wt%)	Biodiesel yield (%)
1	353	20	13	2	3.0
2	353	30	15	4	8.8
3	353	40	17	6	5.8
4	373	20	15	6	77.0
5	373	30	17	2	80.8
6	373	40	13	4	82.8
7	393	20	17	4	73.8
8	393	30	13	6	78.4
9	393	40	15	2	79.3
K_1	6.47	56.60	60.40	60.33	
K_2	88.53	61.80	60.77	60.87	
K_3	85.20	61.80	59.03	59.30	
R	82.07	5.20	1.73	1.57	

mathematical statistical method, unlike the signal factor experiments. Thus, an additional experiment was performed to examine the optimal level. Biodiesel yield of 83.5% was achieved at the optimized conditions, which was higher than the highest yield level of 82.8% in orthogonal table ($A_2B_3C_1D_2$).

3.4.4. Transesterification of *Jatropha* oil over $CaFe_2O_4$–$Ca_2Fe_2O_5$–Fe_3O_4–Fe

Recently, many researchers use nonedible *Jatropha* oil for the production of biodiesel to replace soybean oil [8,10,17]. Raw *Jatropha* oil mainly contains triglycerides of palmitate acid, stearate acid, oleate acid and linoleate acid that also exist in soybean oil. However, raw *Jatropha* oil contains a large portion of free fatty acids, which mainly appear in soybean oil as triglyceride form. This difference contributes to the high acid value in raw *Jatropha* oil, which is harmful to the reactions of *Jatropha* oil. However, in the transesterification of these triglycerides with the carbon number of 16–20, no remarkable difference was found in the chemical reactivity between pretreated *Jatropha* oil and soybean oil. As a result, the biodiesels obtained from pretreated *Jatropha* oil and soybean oil have similar compositions of methyl esters (Fig. S4). Thus, the reaction parameters optimized for soybean oil are directly used in the catalytic transesterification of *Jatropha* oil in this work. But, the direct transesterification of *Jatropha* oil at the same catalysis conditions is not satisfactory. Transesterification of crude *Jatropha* oil over 4 wt% $CaFe_2O_4$–$Ca_2Fe_2O_5$–Fe_3O_4–Fe catalyst gave low biodiesel yield of 3.3% at 373 K for 30 min (Table 3). High acid value of crude *Jatropha* oil resulted in saponification with catalyst, which led to low biodiesel yield [8]. Crude *Jatropha* oil (200 mL) was pretreated with 40 mL methanol over 2 vol% H_2SO_4 at 318 K in an ultrasonic cleaner for 90 min at ultrasonic power 300 W [28]. The acid value of *Jatropha* oil decreased from 12.8 to 1.4 mg/g KOH. The pretreated oil was used in $CaFe_2O_4$–$Ca_2Fe_2O_5$–Fe_3O_4–Fe catalyzed transesterification under the optimized conditions, with biodiesel yield of 78.2% obtained (Table 3).

3.4.5. Recycle of $CaFe_2O_4$–$Ca_2Fe_2O_5$–Fe_3O_4–Fe catalyst

The reduced catalyst can be easily separated by a magnet after transesterification for recycles (Fig. 7). The recycle of the catalyst was studied for the catalytic transesterification of soybean oil under the optimal conditions. Biodiesel yield decreased from 83.5% to 80.4%, 68.3% and 21.7% at the second, third and fourth catalytic cycle, respectively. The deactivation of catalyst was attributed to the loss of active sites through the leaching of Ca. After $CaFe_2O_4$–$Ca_2Fe_2O_5$–Fe_3O_4–Fe catalyst was reused for two times, the surface Ca/Fe molar ratio remarkably decreased from 0.35 to 0.27 (Table 1). Another evidence for the leaching of Ca in the reactions came from the EDX analysis of carbonized biodiesel and glycerol phase after the transesterification (Fig. S5). Considerable amount of Ca was detected from both carbonized chars of biodiesel and glycerol phase, which was believed as the results of Ca leaching during the reactions. The recycle of heterogeneous catalyst was performed with soybean oil. However, similar problems such as the leaching of active components were also seen for *Jatropha* oil transesterification as reported before [28]. Therefore, more efforts are still needed to enhance the activity and thermal stability of $CaFe_2O_4$–$Ca_2Fe_2O_5$-based catalysts in future, which could provide a more satisfactory process economics for the catalytic transesterification.

Table 3
Transesterification of soybean and *Jatropha* oils with magnetic $CaFe_2O_4$–$Ca_2Fe_2O_5$–Fe_3O_4–Fe catalyst.

Materials	Reaction condition	Biodiesel yield (%)
Soybean oil	Reaction temperature of 373 K,	83.5
Crude *Jatropha* oil	reaction time of 30 min,	3.3
Pretreated *Jatropha* oil	methanol/oil molar ratio of 15/1,	78.2
	catalyst amount of 4 wt.%	

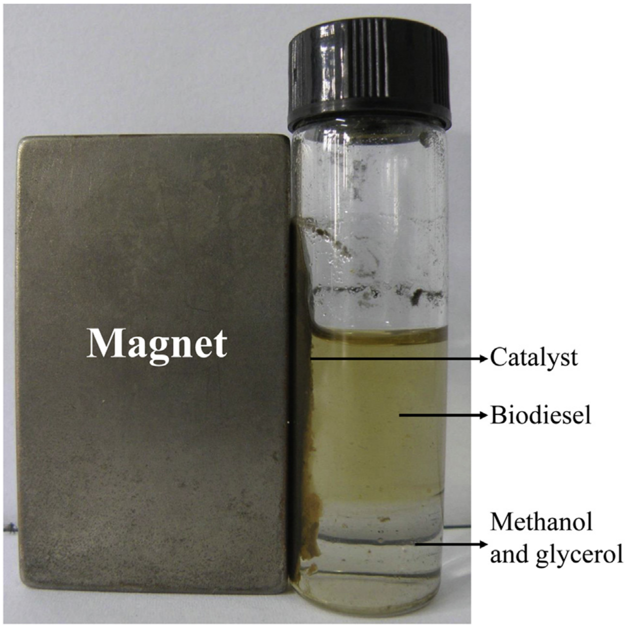

Fig. 7. Image of magnetic $CaFe_2O_4$–$Ca_2Fe_2O_5$–Fe–Fe_3O_4 catalyst separated from biodiesel products by a magnet.

4. Conclusions

Heterogeneous $CaFe_2O_4$–$Ca_2Fe_2O_5$-based catalysts were synthesized by co-precipitation and calcination. The prepared catalyst was composed of crystalline $CaFe_2O_4$, $Ca_2Fe_2O_5$ and Fe_2O_3 ($CaFe_2O_4$–$Ca_2Fe_2O_5$–Fe_2O_3). The $CaFe_2O_4$–$Ca_2Fe_2O_5$–Fe_2O_3 catalyst had strong acid and basic sites to catalyze biodiesel production effectively, and the active components were regarded as mainly $CaFe_2O_4$. A maximum biodiesel yield of 85.4% was achieved under the best conditions (373 K, 30 min, methanol/oil molar ratio of 15/1 and catalyst of 4 wt%). The magnetism of catalyst was strengthened by the reduction of $CaFe_2O_4$–$Ca_2Fe_2O_5$–Fe_2O_3 to new crystalline phase $CaFe_2O_4$–$Ca_2Fe_2O_5$–Fe_3O_4–Fe under H_2 atmosphere. The reduced catalyst had good performance in the catalytic transesterification of soybean oil and pretreated *Jatropha* oil, with the highest biodiesel yield of 83.5% and 78.2%, respectively. The effects of reaction variables on biodiesel yield from soybean oil were optimized by orthogonal experiments, and the optimized conditions were the same to that with $CaFe_2O_4$–$Ca_2Fe_2O_5$–Fe_2O_3 catalyst. Reaction temperature and time had the most significant influence on biodiesel yields, while the impact of methanol to oil molar ratio and catalyst amount was not significant. The two solid catalysts could be recycled three times.

Acknowledgments

The authors wish to acknowledge the financial support from Chinese Academy of Sciences [Bairenjihua, CAS 135 program (XTBG-T02) and equipment R&D grant (No. YZ201260)], the Yunnan Provincial Government (Baiming Haiwai Gaocengci Rencai Jihua), and the Natural Science Foundation of China (No. 21076220). Thanks are also given to the biogeochemical laboratory of Xishuangbanna Tropical Botanical Garden for ICP analysis, and Dr. Lin Lin and Miss Wenyu Wu (Jiangsu University) for VSM analysis.

Appendix A. Supplementary data

Supplementary data related to this article can be found at http://dx.doi.org/10.1016/j.energy.2014.02.082.

References

[1] Lin CY, Cheng HH. Application of mesoporous catalysts over palm-oil biodiesel for adjusting fuel properties. Energy Convers Manage 2012;53:128–34.
[2] Macor A, Pavanello P. Performance and emissions of biodiesel in a boiler for residential heating. Energy 2009;34:2025–32.
[3] Gui MM, Lee KT, Bhatia S. Feasibility of edible oil *vs.* non-edible oil *vs.* waste edible oil as biodiesel feedstock. Energy 2008;33:1646–53.
[4] Deng X, Fang Z, Liu YH. Ultrasonic transesterification of *Jatropha curcas L.* oil to biodiesel by a two-step process. Energy Convers Manage 2010;51:2802–7.
[5] Hanh HD, Dong NT, Okitsu K, Nishimura R, Maeda Y. Biodiesel production through transesterification of triolein with various alcohols in an ultrasonic field. Renew Energy 2009;34:766–8.
[6] Boey PL, Maniam GP, Hamid SA. Performance of calcium oxide as a heterogeneous catalyst in biodiesel production: a review. Chem Eng J 2011;168:15–22.
[7] Li YH, Qiu FX, Yang DY, Li XH, Sun P. Preparation, characterization and application of heterogeneous solid base catalyst for biodiesel production from soybean oil. Biomass Bioenergy 2011;35:2787–95.
[8] Endalew AK, Kiros Y, Zanzi R. Heterogeneous catalysis for biodiesel production from *Jatropha curcas* oil (JCO). Energy 2011;36:2693–700.
[9] Gomes JFP, Puna JFB, Gonçalves LM, Bordado JCM. Study on the use of MgAl hydrotalcites as solid heterogeneous catalysts for biodiesel production. Energy 2011;36:6770–8.
[10] Lee HV, Taufiq-Yap YH, Hussein MZ, Yunus R. Transesterification of *jatropha* oil with methanol over Mg-Zn mixed metal oxide catalysts. Energy 2013;49:12–8.
[11] Hu SY, Guan YP, Wang Y, Han HY. Nano-magnetic catalyst KF/CaO-Fe_3O_4 for biodiesel production. Appl Energy 2011;88:2685–90.
[12] Liu C, Lv PM, Yuan ZH, Yan F, Luo W. The nanometer magnetic solid base catalyst for production of biodiesel. Renew Energy 2010;35:1531–6.
[13] Lin L, Li XQ, Cui FJ, Zhou HN, Shen XQ, Dong MD. Transesterification of rapeseed oil to biodiesel on CaO/α-Fe hollow fiber catalyst: optimization by response surface methodology. Bioenergy Res 2012;5:949–57.
[14] Kouzu M, Hidaka JS. Transesterification of vegetable oil into biodiesel catalyzed by CaO: a review. Fuel 2012;93:1–12.
[15] Liu XJ, He HY, Wang YJ, Zhu SL, Piao XL. Transesterification of soybean oil to biodiesel using CaO as a solid base catalyst. Fuel 2008;87:216–21.
[16] Zabeti M, Daud WMAW, Aroua MK. Biodiesel production using alumina-supported calcium oxide: an optimization study. Fuel Process Technol 2010;91:243–8.
[17] Taufiq-Yap YH, Lee HV, Hussein MZ, Yunus R. Calcium-based mixed oxide catalysts for methanolysis of *Jatropha curcas* oil to biodiesel. Biomass Bioenergy 2011;35:827–34.
[18] Ullah K, Ahmad M, Sultana S, Teong LK, Sharma VK, Abdullah AZ, et al. Experimental analysis of di-functional magnetic oxide catalyst and its performance in the hemp plant biodiesel production. Appl Energy 2014;113:660–9.
[19] Hájek M, Skopal F, Čapek L, Černoch M, Kutálek P. Ethanolysis of rapeseed oil by KOH as homogeneous and as heterogeneous catalyst supported on alumina and CaO. Energy 2012;48:392–7.
[20] Kouzu M, Yamanaka SY, Hidaka JS, Tsunomori M. Heterogeneous catalysis of calcium oxide used for transesterification of soybean oil with refluxing methanol. Appl Catal A 2009;355:94–9.
[21] Zouari S, Ranno L, Cheikh-Rouhou A, Isnard O, Wolfers P, Bordet P, et al. Structural and magnetic properties of the $(Ca_{1-x}Na_x)(Fe_{2-x}Ti_x)O_4$ solid solution $(0 \leq x \leq 1)$. J Alloys Compd 2008;452:234–40.
[22] Hirabayashi D, Yoshikawa T, Mochizuki K, Suzuki K, Sakai Y. Formation of brownmillerite type calcium ferrite ($Ca_2Fe_2O_5$) and catalytic properties in propylene combustion. Catal Lett 2006;110:269–74.
[23] Pardeshi SK, Pawar RY. Optimization of reaction conditions in selective oxidation of styrene over fine crystallite spinel-type $CaFe_2O_4$ complex oxide catalyst. Mater Res Bull 2010;45:609–15.
[24] Kawashima A, Matsubara K, Honda K. Development of heterogeneous base catalysts for biodiesel production. Bioresour Technol 2008;99:3439–43.
[25] Guo F, Peng ZG, Dai JY, Xiu ZL. Calcined sodium silicate as solid base catalyst for biodiesel production. Fuel Process Technol 2010;91:322–8.
[26] Xie WL, Peng H, Chen LG. Calcined Mg-Al hydrotalcites as solid base catalysts for methanolysis of soybean oil. J Mol Catal A Chem 2006;246:24–32.
[27] Long YD, Guo F, Fang Z, Tian XF, Jiang LQ, Zhang F. Production of biodiesel and lactic acid from rapeseed oil using sodium silicate as catalyst. Bioresour Technol 2011;102:6884–6.
[28] Deng X, Fang Z, Liu YH, Yu CL. Production of biodiesel from *Jatropha* oil catalyzed by nanosized solid basic catalyst. Energy 2011;36:777–84.
[29] Wang JH, Tao ZC, Yang Y, Chang J, Xiang HW, Li YW. Reduction kinetics of α-Fe_2O_3 microspheres. Chin J Process Eng 2007;7:288–92 [Chinese].
[30] Hou BL, Zhang HY, Li HZ, Zhu QS. Study on kinetics of iron oxide reduction by hydrogen. Chin J Chem Eng 2012;20:10–7.
[31] Pandey SK, Bindu R, Bhatt P, Chaudhari SM, Pimpale AV. Synthesis and investigation of structural and electronic properties of $Pr_{1-x}Ca_xFeO_3$ $(0 \leqq x \leqq 0.2)$ compounds. Physica B 2005;365:47–54.
[32] Wagner CD, Riggs WM, Davis LE, Moulder JF, Muilenberg GE. Handbook of X-ray photoelectron spectroscopy. 1st ed. Eden Prairie, Minnesota: Perkin-Elmer corporation; 1979.
[33] Khachani M, Kacimi M, Ensuque A, Piquemal JY, Connan C, Bozon-Verduraz F, et al. Iron–calcium–hydroxyapatite catalysts: Iron speciation and comparative performances in butan-2-ol conversion and propane oxidative dehydrogenation. Appl Catal A 2010;388:113–23.